Bull. Soc. géol. France, 2002, t. 173, n° 5, pp. 437-448

Role of an extension of pre-Quaternary age for the evolution of the carbonate massifs in the occidental Betic Cordillera : The case of the Yunquera-Nieves massif (southern Spain)

SÉVERIN PISTRE[1], CRISTINA LIÑÁN[2], BARTOLOMÉ ANDREO[2], FRANCISCO CARRASCO[2], CLAUDE DROGUE[1] and AGUSTÍN MARTIN-ALGARRA[3]

Key words. – Betic Cordillera, Yunquera-Nieves unit, Karst, Fracturation, Paleo-stress fields, Extension, pre-Quaternary.

Abstract. – A simultaneous analysis of the fracture geometry and paleo-stress fields of the karstic Yunquera-Nieves massif in southern Spain (Málaga Province) has been carried out with microtectonic stations. It reveals polyphased tectonics linked to the structural position of this carbonate domain in the western Betic Cordillera.

Among the tectonic regimes described in this domain appears a distensive stage with a radial trend probably of post-Tortonian to Quaternary age. Todate, it has seldom been described and is absent from geodynamic models though it seems to have had a regional importance. Furthermore, it played a major role for the acquisition of the hydrodynamic properties of the aquifer and its karstogenesis. This stage opened all fractures and allowed the development of karstic drains with NW-SE and N-S directions. Finally, the karstic network was shaped by more recent climatic and tectonic events.

Rôle d'un régime extensif pré-quaternaire dans l'évolution des massifs carbonatés de la Cordillère bétique occidentale : exemple du massif de Yunquera-Nieves (Sud de l'Espagne)

Mots clés. – Cordillère Bétique, Unité Yunquera-Nieves, Karst, Fracturation, Paléochamps de contraintes, Extension, Pré-Quaternaire.

Résumé. – **Introduction.** – Le contexte géodynamique particulier de la partie ouest de la Méditerranée a suscité de nombreux travaux [Taponnier, 1977; Dercourt *et al.*, 1986; Martín-Algarra, 1987; Sanz de Galdeano, 1990]. Ceux-ci ont montré un polyphasage tectonique complexe depuis le Crétacé lié aux mouvements relatifs de l'Afrique et de la péninsule ibérique. Les différents stades tectoniques ont contrôlé la genèse et l'évolution des réseaux fissurés ainsi que leur karstification en domaine carbonaté : l'unité de Yunquera-Nieves qui est située dans la Province de Malaga, fournit un exemple de massif karstique à fort potentiel d'exploitation hydrique. La caractérisation de sa structure géologique et de son réseau fissural doit permettre d'une part de préciser l'allure et l'évolution des champs de contraintes dans cette partie de la chaîne, d'autre part de fournir des éléments d'ordre méthodologique relatifs à l'estimation des ressources aquifères des karsts fortement tectonisés.

L'unité de Yunquera-Nieves. – L'unité de Las Nieves qui constitue la majeure partie de l'aire d'étude fait partie du Rondaide (fig. 1). Elle chevauche le Pénibétique. Elle-même est chevauchée par l'Alpujarride représenté en grande partie par des péridotites et par le Malaguide (fig. 2). Une des unités chevauchantes est l'unité de Yunquera qui affleure dans la partie est de l'aire d'étude [Martín-Algarra, 1987]. La structure géologique de l'unité de Las Nieves correspond à un synclinal couché vers le NW, dont le flanc sud renversé est affecté par un métamorphisme de contact (fig. 2). L'unité de Yunquera présente une structure monoclinale vers le Nord à anticlinale vers l'Est. La structure géologique décrite est affectée par des failles transversales (en particulier NW-SE), qui compartimente le massif.

La séquence stratigraphique de l'unité de Las Nieves [Dürr, 1967 ; Bourgois, 1978 ; Martín-Algarra, 1987] montre une épaisse série carbonatée (1 600 m) qui contient les termes suivants : dolomies du Norien avec une épaisseur supérieure à 1 000 m ; calcaires et marno-calcaires du Rhétien ; calcaires à silex du Lias inférieur ; calcaires parfois marneux à nodules, radiolarites et marnes attribuées à la séquence Jurassique-Tertiaire ; brèche de la Nava d'âge Aquitanien et syn à post-plissement [Martín-Algarra et Estévez, 1984].

La séquence stratigraphique de l'unité de Yunquera est formée par trois sous-ensembles lithologiques dont l'inférieur comporte plus de 300 mètres de métapélites, gneiss et micaschistes du Paléozoïque et du Trias inférieur. Le sous-ensemble intermédiaire est formé par des marbres dolomitiques du Trias moyen, et le supérieur par des calcaires et des calcoschistes du Trias supérieur.

Analyse de la fracturation. – A l'échelle du massif, la fracturation a été analysée à partir de photos aériennes pour dessiner une carte de plus de 600 linéaments. A l'échelle de l'affleurement, la fracturation a été analysée à partir de 38 stations microtectoniques. Les paramètres observés étaient la direction, le pendage, l'espacement et la qualité de ces

[1] CNRS UMR 5569, Laboratoire Hydrosciences, Institut des Sciences de la Terre de l'Eau et de l'Espace de Montpellier, Université Montpellier 2, 34095 Montpellier cedex 05, France. pistre@msem.univ-montp2.fr
[2]Departamento de Geología, Facultad de Ciencias, Universidad de Málaga, 29071 Málaga, Spain.hidrogeo@uma.es
[3]Departamento de Estratigrafia, Facultad de Ciencias, Universidad de Granada, 18071 Granada, Spain.hidrogeo@uma.es
Manuscrit déposé le 25 juillet 2001 ; accepté après révision le 17 avril 2002.

discontinuités. Une attention particulière a été portée aux failles sur lesquelles, en plus des paramètres précédents, les stries ont été mesurées. Elles ont été traitées par la méthode inverse d'Etchécopar [Etchécopar *et al.*, 1981] et par une méthode directe basée sur le concept des contraintes optimales [Bott, 1959].

La fracturation kilométrique (fig. 3A) est organisée selon 2 directions mal définies WSW-ESE et NW-SE alors que les failles normales sont mieux organisées dans ces directions (fig. 3B). Pour la fracturation de plus petite dimension, les familles principales sont N135-165 et N000 qui est souvent karstifiée alors que les failles secondaires sont N060-070 et E-W qui est la seule à être rarement karstifiée (fig. 4 et fig. 5). Toutes les familles possèdent des failles normales alors que les failles inverses sont plutôt NW-SE (fig. 6).

L'analyse des mesures de stries sur l'ensemble des stations montre un polyphasage clair (fig. 7). Deux tenseurs mal contraints ressortent (fig. 8 et fig. 9) :
– un tenseur décrochant (TINV65) à $\sigma 1$ N150 défini à partir de 65 % des failles inverses
– un tenseur extensif (TNORM60) à $\sigma 3$ N055 défini à partir de 60 % des failles normales.

TNORM qui est très similaire au tenseur défini à partir de 35 % de l'ensemble des failles (TOUT35) se rencontre sur la plupart des stations contrairement à TINV65 (fig. 8). D'après les observations de stries sécantes, TNORM60 paraît plus récent que TINV65.

La figure 10 montre la méthode utilisée pour caractériser une station en prenant l'exemple d'une station comportant un critère chronologique. Dans ce cas, une strie (n° 25) expliquée par le tenseur décrochant est antérieure à une strie (n° 26) expliquée par le tenseur extensif. L'analyse des stries sur chaque station (fig. 11) fournit deux types de tenseurs comparables à TINV65 et TNORM60 qui apparaît avec une tendance radiale.

Intégration des résultats dans le contexte géodynamique régional. – La situation de l'unité de Yunquera-Nieves dans la partie occidentale de la Cordillère bétique lui confère une histoire tectonique complexe liée aux mouvements relatifs irréguliers de l'Afrique et de la Péninsule ibérique. Depuis le Jurassique, la convergence de l'Afrique vers l'Europe crée une situation globalement compressive contrôlée par la subduction de l'Afrique et l'ouverture du bassin algéro-provençal [Robertson et Grasso, 1995]. Elle se traduit par la déformation progressive du domaine bétique marquée par la collision au Burdigalien entre les zones internes (Z.I.) et zones externes (Z.E.) : la direction de la compression est alors NW-SE [Sanz de Galdeano, 1990]. Après la suture du contact entre Z.I. et Z.E., la direction de compression devient WNW-ESE au Serravalien et pivote à nouveau pour devenir NNW-SSE au Tortonien (à Messinien) en régime décrochant [Ott d'Estevou et Montenat, 1985]. Le premier régime trouvé dans l'Unité de Yunquera-Nieves est cohérent avec cette phase.

De la fin du Miocène au début du Quaternaire, le régime tectonique est débattu. Il était considéré comme globalement extensif [Benkhelil, 1976 ; Groupe de Recherche Néotectonique de l'Arc de Gibraltar, 1977] avec une distension environ N-S [Benkhelil et Guiraud, 1976]. Mais plus récemment certains auteurs [Ott d'Estevou et Montenat, 1985 ; Simon-Gómez, 1986] ont indiqué pour la même période un régime caractérisé par une compression N-S et une extension perpendiculaire ou par une extension radiale dans certains secteurs [Jalaboy *et al.*, 1993]. Celle-ci a été notée dans la région de Granada, sur les pentes de la Sierra Nevada [Galindo-Zaldívar et González-Lodeiro, 1988] ou en bordure du bassin de Granada [Pistre *et al.*, 1999]. Le deuxième régime trouvé dans l'unité de Yunquera-Nieves est cohérent avec cette phase et est compatible avec les mesures de Andreo *et al.* [1997] sur le complexe carbonaté voisin formé par les Sierras Blanca et Mijas.

D'après la plupart des auteurs, à partir du début du Pléistocène, un régime peu intense s'installe d'abord décrochant [Bousquet et Philip, 1976b] puis franchement compressif avec une direction de raccourcissement proche de N-S. Ce régime semble correspondre au régime actuel. Toutefois un régime distensif post-Quaternaire moyen comparable à celui post-tortonien à quaternaire a localement été signalé avec une intensité plus faible [Lhénaff, 1965 ; Sanz de Galdeano, 1980].

Conséquences sur les écoulements souterrains. – Les phases orogéniques intenses miocènes ont permis l'individualisation du massif et sa structuration générale achevée à l'Aquitanien/Burdigalien comme en témoignent les brèches de la Nava. Sa position structurale chevauchante sur les matériaux pénibétiques peu perméables, bordée du sud à l'est par des terrains alpujarrides (péridotites) et malaguides (flysch) explique la direction générale des écoulements et la position des sources [Liñán *et al.*, 1996].

A l'intérieur du massif, la fracturation est probablement héritée en grande partie des premiers stades orogéniques. L'ensemble carbonaté de Yunquera-Nieves a certainement aquis l'essentiel de ses propriétés aquifères lors de l'épisode distensif mis en évidence dont la direction d'extension est autour de NE-SW mais qui possède une tendance radiale. Ce régime semble post-tortonien et ante-quaternaire car les régimes qui ont suivi ne paraissent pas suffisament intenses pour déformer de façon sensible l'intérieur des compartiments. La tendance radiale de ce régime distensif a fait rejouer la plupart des familles directionnelles de joints préexistants créant une perméabilité d'ensemble importante.

Ces résultats précisent les quatre étapes de karstification post-burdigaliennes de Delannoy et Guendon [1998].
– La période post-Burdigalien à ante-Messinien correspond au développement d'un karst de faible énergie.
– Au Messinien, l'effet combiné de la baisse du niveau eustatique et de la mise en place d'un régime distensif accélère la karstification et permet le développement de structures verticales. A l'intérieur du massif, cela se traduit par le développement de drains NW-SE et subméridiens (perpendiculaires à la contrainte mineure NE-SW). Eux-mêmes contrôlent la karstification de la fracturation métrique ou décamétrique qui s'est développée dans toutes les directions.
– La transgression pliocène ralenti la karstification en relevant le niveau de base hydraulique.
– Lors des périodes quaternaires, la karstification est contrôlée par des processus tectoniques et surtout climatiques ou anthropiques par modification du couvert végétal [Delannoy, 1997] comme en témoigne la succession des dépôts travertineux [Durán-Valsero, 1996].

Conclusion. – Dans le massif de Yunquera-Nieves, l'analyse conjointe du réseau fissuré et des paléochamps de contraintes a permis d'établir le rôle de la tectonique dans son évolution karstique. Un régime extensif récent à tendance radiale a été mis en évidence de manière claire. Ce résultat a une incidence importante sur le schéma géodynamique de la

partie occidentale de la Cordillère bétique ; il pourrait indiquer un réajustement isostatique post-orogénique régional.

A l'intérieur du massif, ce régime a induit le développement d'une structure multi-porosité typiquement karstique avec de grands drains (NW-SE et subméridiens) alimentés par un réseau de plus petite échelle (fracturation NW-SE et subméridienne mais aussi E-W et NE-SW).

D'un point de vue méthodologique dans l'approche des réservoirs carbonatés en domaines fortement tectonisés, ces résultats montrent l'influence des régimes tectoniques régionaux sur les circulations souterraines d'échelle plus locale.

INTRODUCTION

Since the Cretaceous, the occidental part of the Mediterranean basin is the scene of important geodynamic processes which are essentially related to movements of the African continent [Tapponnier, 1977; Dercourt *et al*., 1986; Martín-Algarra, 1987; Sanz de Galdeano, 1990; Robertson and Grasso, 1995]. Studies carried out in different sectors of the Betic Cordillera permitted to become acquainted with the spatial and temporal variation of tectonic constraints and describe the characteristics of the deformation at a local as well as a regional scale [Benkhelil, 1976; Bousquet, 1979; Sanz de Galdeano, 1983]. If all reveal a complex polyphasing dominated by compressive regimes, certain studies state more or less marked and hence often discussed distensive regimes from the Miocene onwards [Groupe de Recherche néotectonique de l'Arc de Gibraltar, 1977; Vissers and Van der Wal, 1993; Crespo-Blanc *et al.*, 1994].

From an applied point of view, the knowledge of the fracturing and its evolution, in particular during recent periods, is essential for the exploitation of subterranean water resources in a carbonate domain [Kiraly, 1975; Drogue *et al.*, 1975; Grillot, 1979; Ford and Williams, 1989]. Fracturing controls the aquifers geometry and their karstification. The role played by each tectonic episode is generally delicate to estimate even though it is fundamental regarding the acquisition of karstic properties [Drogue and Costa Almeida, 1984; Quinif *et al*., 1997].

Located west of Malaga within the Serrania de Ronda, the carbonate unit of Yunquera-Nieves constitutes an example for a karstic reservoir in the occidental part of the Betic Cordillera. From east to west, it is composed of the Sierras de Las Nieves, Yunquera, Prieta and Alcaparaìn. The characterisation of its geological structure and fracture network should allow, first, to precise the aspect and the evolution of the stress fields in this part of the range, and second, to provide methodological elements relative to the estimation of aquifer resources of highly tectonized karsts.

THE YUNQUERA-NIEVES UNIT

Structural context

In the Betic Cordillera, the external zone corresponds to the south Iberian paleo-margin during the Mesozoic and the Tertiary. North of the region studied, it is represented by its most internal domain (Penibetic). The Betic internal zone is formed by several flaked and superposed tectonic complexes including, in ascending order, the Alpujarride or Rondaide in the occidental part of the Cordillera and the Malaguide (fig. 1).

The geological description of the study area (fig. 2) has been carried out by a number of geologists of which shall be cited Blumenthal [1930] who defined the Rondaide, Dürr [1967] who established the geological stratigraphy and the cartography of the Sierras de Las Nieves and Cabrilla, Bourgois [1978] who did the same for the Sierras Prieta and Alcaparaín, and Martín-Algarra [1987] who improved and unified the criteria of anterior authors for the entire Yunquera-Nieves unit formed by the Sierras de Las Nieves, Yunquera, Prieta, and Alcaparaín.

Based on previous work it is possible to differentiate two tectonic units which are separated by an overthrusting contact : the Las Nieves unit, in low position, which shows Rondaide affinities (according to Blumenthal [1930], Hoeppener *et al.*, [1964], Dürr [1967], Martín-Algarra [1987]), and the Yunquera unit with Alpujarride affinities [Dürr, 1967; Martín-Algarra, 1987]. The Las Nieves unit outcrops throughout the entire area studied whereas the Yunquera unit appears only in the central and oriental zones.

Stratigraphic series

The stratigraphic series as described by Dürr [1967], and more in detail by Martín-Algarra [1987] shows an essentially carbonate composition for a thickness of 1 600 metres. It contains the following terms (fig. 2) :

– the most important term of the series is the inferior term, formed by Norian dolomites, of a thickness which can exceed 1 000 metres ;

– above, one finds 200 metres of black limestone with layers of calcareous marls from the Rhetian and 150 metres of flint limestones from the early Lias ;

– a condensed sequence (50 m width) follows, which corresponds to the period from the Jurassic to Tertiary, composed of limestones, which are sometimes marly and knobly, as well as radiolarites and marls ;

– discordant on the preceding terms, the breccias of La Nava appears to be of Aquitanian age, probably final Aquitanian [Martín-Algarra et Estévez, 1984] ;

The stratigraphic sequence of the Yunquera unit is formed by three lithological subsets :

– the inferior comprises more than 300 metres of metapelites, gneiss, and micaschist (the Yunquera formation) from the Palaeozoic and lower Triassic ;

– the intermediate subset is formed by dolomitic marbles of the mid Triassic, progressively less metamorphic towards the formation top (the Carratraca formation) ;

– the top set is composed of limestone and calcareous schists (the Capellan formation) of the upper Triassic, the latter augmenting in proportion towards the summit.

Geological structure

The Las Nieves unit, which constitutes the major part of the study area, overthrusts the Penibetic. Between both lies a strip of materials corresponding to the flysch of the Campo

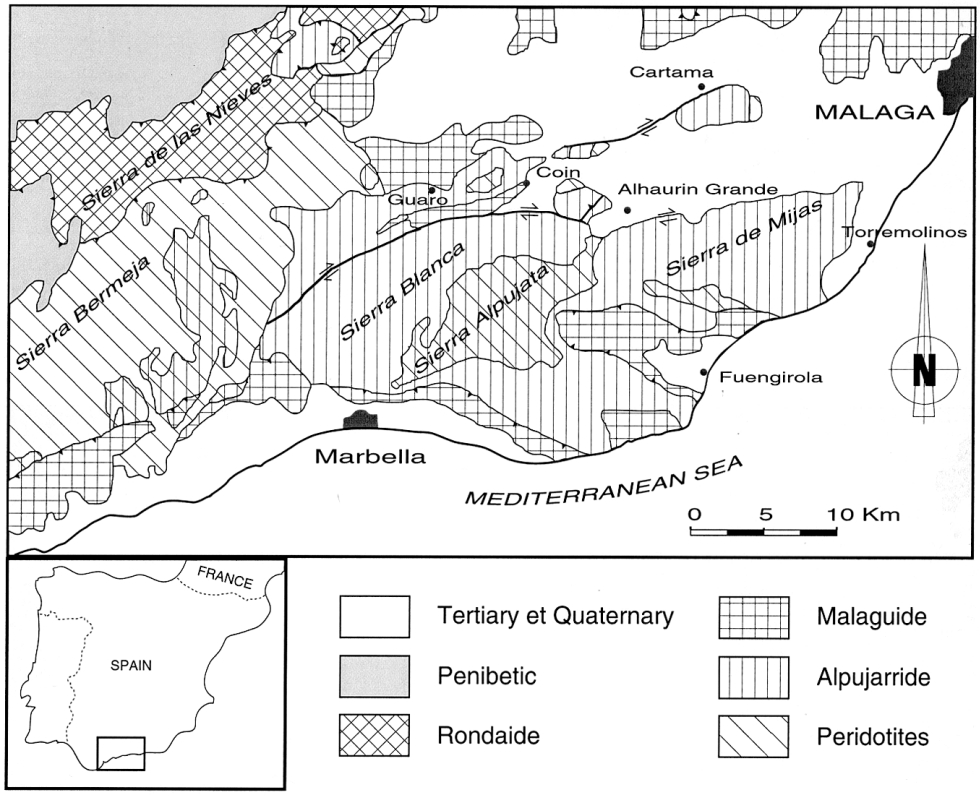

FIG. 1. – Position and structural context of the Yunquera-Nieves unit (from Andreo *et al*. [1997]).
FIG. 1. – *Localisation et contexte structural de l'unité de Yunquera-Nieves (d'après Andreo* et al. *[1997]).*

de Gibraltar. It is itself overthrusted by the Alpujarride which is represented to a large part by peridotites, and the Malaguide. One of the overthrusting units is the Yunquera unit which appears in the eastern part of the study area.

The geological structure of the Las Nieves unit corresponds to a synclinal overturned north-westwards, whose southern inverse slope is affected by a contact metamorphism linked to overthrusting peridotites of the Las Reales unit (fig. 2). The orientation of the fold varies from N040-060 E in the sector of the Torecilla peak to almost N-S in the Sierras Prieta and Alcaparaín. The structure is particularly visible in the occidental part. On the other hand, the inverse slope is flaky in the sector of the Torecilla peak, while the structure is "duplicated" in the Sierras Prieta and Alcaparaín (fig. 2).

The Yunquera unit, west and north-west of the village Yunquera, presents a monoclinal structure towards the north, whereas it is of anticlinal aspect in the east and northeast. On the southern slope of the Sierra Prieta, the dip is south, with a tendency to verticalisation, like in the Sierra Alcaparaín.

The Las Navas breccias are implicated to the structure as a part of it has been deposited prior to the final structuring of the Las Nieves unit, while another part has been deposited after the overthrusting of the Yunquera unit [Martín-Algarra and Estévez, 1984]. The breccias deposition, however, ended before the Los Reales unit and the Malaguide arose.

The geological structure described above is affected by transversal faults partitioning the massif. In particular, large faults in NW-SE direction play a major role for its morphology.

ANALYSIS OF THE FRACTURING

Methodology

The data on fracturing have two origins, each corresponding to a different observation scale. A field of fractures at the scale of the massif has been drawn after the analysis of aerial photographs (approximately 1/33 000), followed by a check on the ground. It comprises more than 600 lineaments, 147 of which could, based on structural criteria on the ground, be identified as corresponding to the traces of normal faults. For the reason of biases concerning the determinations of length or density of these lineaments due to strong slopes and vegetation contrasts, the analysis has been restricted to a statistical analysis of the directions (fig. 3).

On the other hand, 38 microtectonic stations distributed in a relatively homogeneous manner throughout the massif allowed to measure 316 fractures (*s.l.*) including faults, diaclases, karstified and not karstified joints. At each station, a single fracture has been measured for each of the fracture families in order to avoid certain statistical biases and, chiefly, to avoid bias when determining stress tensors. The parameters measured were direction, rake, spacing and qua-

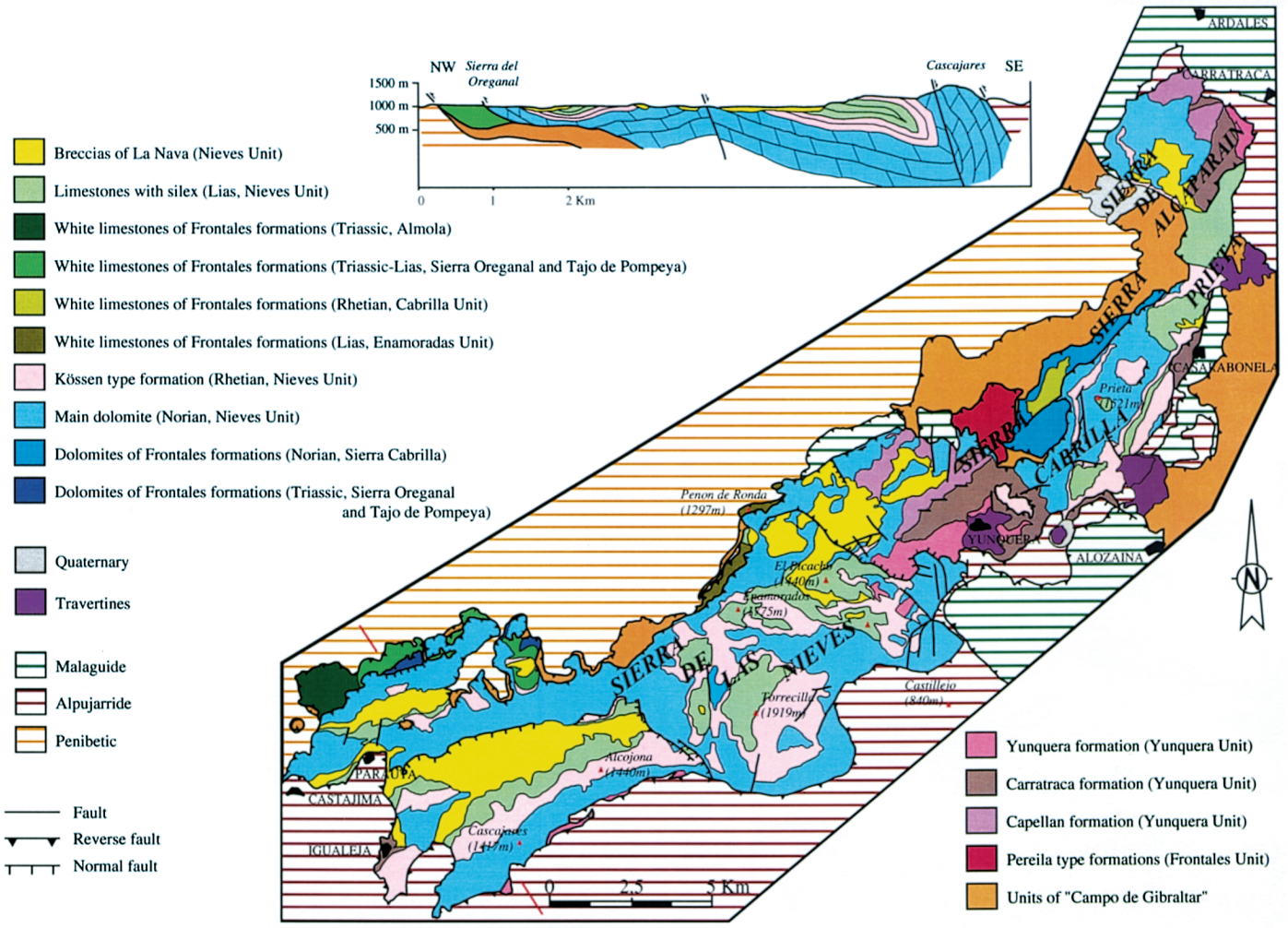

FIG. 2. – Simplified geological map of the Yunquera-Nieves unit (from Martín-Algarra [1987]) and cross-section of the Yunquera-Nieves unit (from Dürr [1967] and Bourgois *et al.* [1978]).
FIG. 2. – *Carte géologique simplifiée de l'unité de Yunquera-Nieves (d'après Martín-Algarra [1987]) et coupe transversale de l'unité de Yunquera-Nieves (d'après Dürr [1967] et Bourgois* et al. *[1978]).*

lity of these discontinuities. Particular attention was paid to the faults, where the pitch and the type of striae, the sense of movement, and relations with other discontinuities were recorded in addition to the preceding parameters : 164 measurements of striae have been retained. The limited access to the interior part of the massif and the frequency of dolomitic or highly karstified facies have nevertheless reduced the opportunities to make observations, in particular of striae.

The analysis of the striae measurements made use of an inverse approach combined with a direct approach. The first, which corresponds to Etchécopar's method [Etchécopar *et al.*, 1981; Ritz, 1991], identifies by a random draw and subsequent regression the tensor which "explains" a striae population best in the sense of optimal constraints [Bott, 1959; Angelier and Goguel, 1979]. In practice, it necessitates at least 6 consistent data to constrain a tensor efficiently. The second, also based on the concept of optimal constraints, calculates either the tensor associated with each striae (for a chosen friction angle of 30°) or the deviation from a given tensor. It doesn't allow to access the ratio R [Célérier, 1995], where $R = (\sigma 2 - \sigma 3) / (\sigma 1 - \sigma 3)$, with $\sigma 1$, $\sigma 2$ and $\sigma 3$ representing the major, intermediate, and minor constraint, respectively.

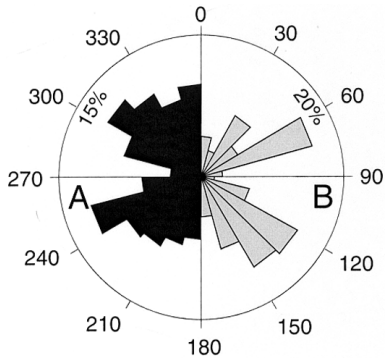

FIG. 3. – Directional fracture histogram from aerial observations at the scale of the massif – A : all fractures (600); B : normal faults (147).
FIG. 3. – *Distribution directionnelle de la fracturation relevée par photographie aérienne à l'échelle du massif* – A *: toutes les fractures (600);* B *: failles normales (147).*

The fractured network

The general fracturing at a kilo to hectometric scale is organized following two directions, WSW-ENE and NW-SE which appear badly defined since numerous classes are

only little less well defined, like e.g. the N-S one (fig. 3A). The WSW-ENE direction is generally also that of the axes of the folds (and that of the stratification). This distribution is close to that observed by Benavente Herrera and Sanz de Galdeano [1985] at a larger scale. The network of the normal faults is better organized according to these same two directions and reveals classes which are very weakly represented, such as the E-W or N-S classes (fig. 3B).

At the scale of the microtectonic stations, i.e. the metric to decametric fracturing, two major directions become clearly apparent when considering the totality of measurements (fig. 5A) : N135 to N165 and N000 to N015, which were not really perceptible at the scale of the massif. Less distinctly, one finds the direction N060 to N075, while a secondary direction N090 to N105 emerges. Except the secondary direction N090 to N105, which disappears, the karstic network of identical scale is retraced along the same directions, with a marked predominance of N000 to N015 planes (fig. 5B). The directional distribution of the normal faults (fig. 6A) resembles strongly that of the karstified planes, even though the direction N090 to N105 is represented. The direction NW-SE seems to emerge for the reverse faults (fig. 6B), but the analysis becomes delicate due to a reduced sample size (40 measurements).

In almost all stations, the NW-SE fractures are organized in often very dense directional families and are regularly found to be open or karstified (fig. 4). At outcrop, the other fracturing directions (N-S and NE-SW) are less frequently encountered in organized families. Their spacing is generally larger or irregular. Fractures belonging to these families are open in some stations, but rarely karstified.

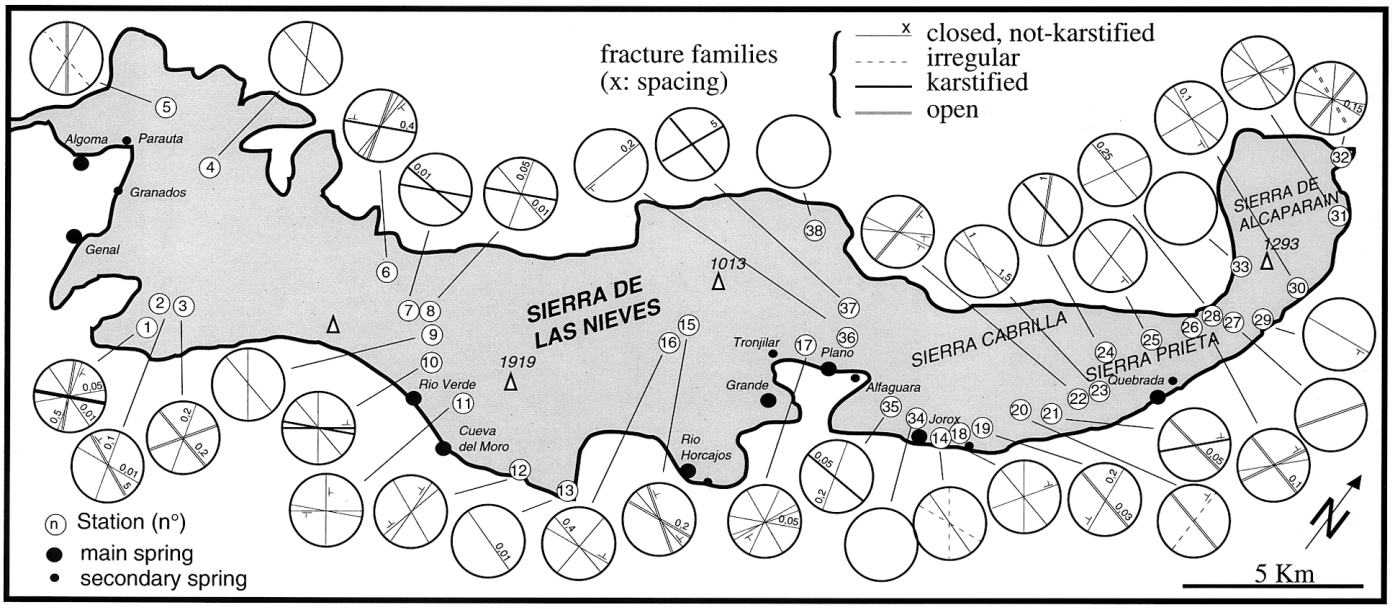

FIG. 4. – Map of microtectonic stations and observed fracture sets (spacing in meters).
FIG. 4. – *Carte des stations microtectoniques et familles de fractures observées par station (espacement en mètre).*

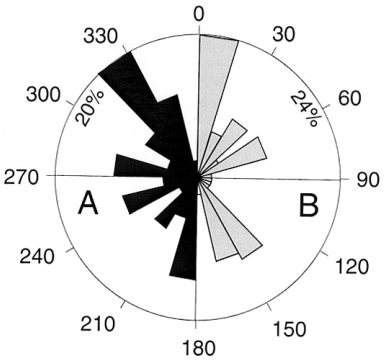

FIG. 5. – Directional fracture histogram from outcrop observations (stations).
A : all fractures (316); B : karstified joints (75)
FIG. 5. – *Distribution directionnelle des fractures mesurées à l'échelle de l'affleurement (stations).*
A : *toutes les fractures (316);* B : *fractures karstifiées (75).*

The paleostress fields

Analysis for the totality of the stations

If one considers the 164 measurements of striated planes, pure reverse faults are rare (10 % of a total 40) and the pure normal faults small in number (37 % of a total 99), which is consistent with the strong rake observed (fig. 7). Furthermore, figure 7A confirms that these generally happen to be due to movements on a pre-existing fracturing and that the new fracture is reduced : indeed, normal faults cannot be grouped in families regarding their direction or rake. These results hence indicate, prior to any determination of a tensor, that the observations of striae correspond to several phases which could have caused several movements along the same plane as it has been noticed in certain favourable cases (two intersecting striae).

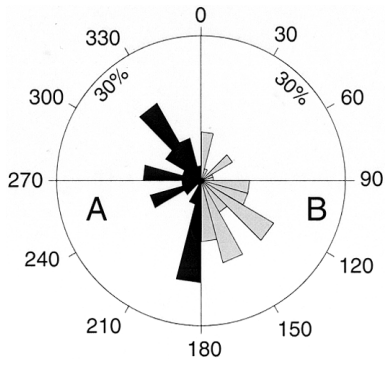

FIG. 6. – Directional fault histogram from outcrop observations (stations).
A : normal faults (90); B : reverse faults (40)
FIG. 6. – *Distribution directionnelle des failles mesurées à l'échelle de l'affleurement (stations).*
A : failles à composante normale (90); B : *failles à composante inverse (40)*

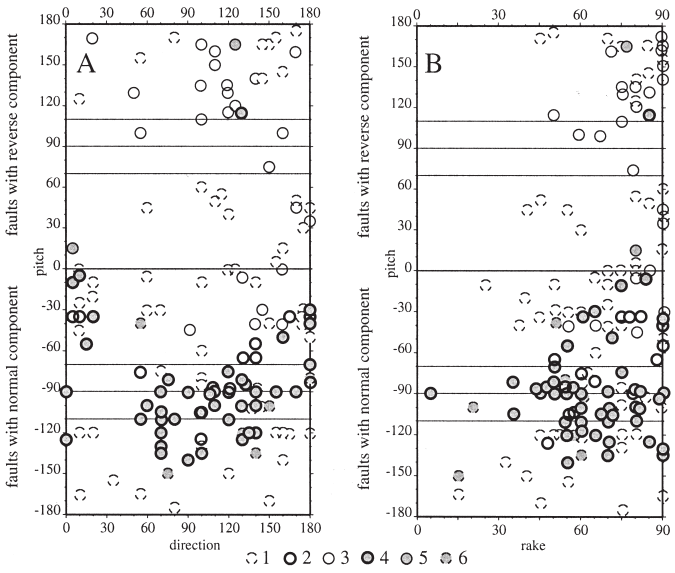

FIG. 7. – Spatial distribution of the striae mesured (146) on the microtectonic stations.
A : pitch/direction diagram
B : pitch/rake diagram: 1 : striae unconsistent with the tensors TOUT35, TNORM60 or TINV65; 2 : striae consistent with the tensor TNORM60; 3 : striae consistent with the tensor TINV65; 4 : striae consistent with the tensors TOUT35 and TNORM60 ; 5 : striae consistent with the tensors TOUT35 and TINV65; 6 : striae consistent with the tensor TINV65 only ; a striae is considered consistent with a tensor when the angle between the computed striae and the observed one is smaller than 30°.
FIG. 7. – *Distribution spatiale des stries mesurées (146) sur les stations microtectoniques.*
A *: diagramme pitch/direction*
B *: diagramme pitch/pendage :* 1 *: stries non expliquées par les tenseurs TOUT35, TNORM60 ou TINV65 ;* 2 *: stries expliquées par le tenseur TNORM60 ;* 3 *: stries expliquées par le tenseur TINV65 ;* 4 *: stries expliquées par les tenseurs TOUT35 et TNORM60 ;* 5 *: stries expliquées par les tenseurs TOUT35 et TINV65 ;* 6 *: stries expliquées par le tenseur TINV65 seulement ; Une strie est dite expliquée par un tenseur pour un écart angulaire entre stries théorique et observée inférieur à 30°.*

Despite this very clear polyphasing, linked to the regional context [Martín-Algarra, 1987; Sanz de Galdeano, 1990], Etchécopar's method allows to identify two tensors which suffice to explain more than half of the faults (fig. 8) :

– TINV65 corresponds to a slightly wrenching regime (R=0.15) defined on the basis of 65 % of the reverse faults (26 faults) with a slightly dipping $\sigma 1$ of direction N150. This tensor explains the striae measured essentially at E-W and NE-SW plane with strong rake (wrenching reverse faults).

– TNORM60 corresponds to an extensive regime defined on the basis of 57 % of the normal faults (56 faults) with a $\sigma 3$ orientated N055 and a vertical $\sigma 1$. The ratio R equals 0.52. The tensor TOUT35 defined on the basis of 35 % of all faults (49 normal faults and 3 reverse faults, or 52 faults overall) is very similar since it is essentially constrained by normal faults. It indicates an extension of a more radial trend (smaller R). The planes concerned have directions corresponding to those shown in figure 6 : there is no privileged direction. The rake of these planes ranges from moderate to strong (purely normal to normal wrenching faults).

These regimes are nevertheless badly constrained and bear important errors for the calculation of the R ratio. The corresponding histograms show irregular deviations between observed and calculated striae. Likely reasons are local effects, among which are local deviations of constraints in proximity of certain accidents.

The definite chronology of these regimes is delicate to establish from the microtectonic data as the cases of intersecting striae are not numerous. Only 3 cases out of 8 observed with anteriority criteria indicate that TINV65 is anterior to TNORM60. In the other cases, at least one stria cannot be explained by one of the two tensors.

The optimal constraint method gives sensibly similar results (fig. 9) with :

– $\sigma 3$ values close to the horizontal of an average direction N045, and moderately to strongly dipping $\sigma 1$ values for normal faults (fig. 9A)

– slightly dipping $\sigma 1$ values with an average direction N150 and close to horizontal $\sigma 3$ values for reverse faults (fig. 9B).

Figure 8 confirms the dominant and non-localised character of the tensor TNORM60. Indeed, and contrasting with tensor TINV65, it is encountered at almost all planes which possess more than two measurements of striae. For the five remaining, the tensor TOUT35 is present at three. Actually, 14 stations possess less than two measured striae, generally because of their position in the dolomites where movement criteria are not visible.

This better visibility of the TNORM60 tensor due to the relative abundance of normal faults is probably due to its posterior character regarding the tensor TINV65. In figure 9, the tensors corresponding to the pairs of intersecting striae (a, a'), (b, b'), (c, c') have been spotted, and a, b, c, are posterior to a', b', c', respectively.

Station-by-station analysis

For half of the stations, an insufficient number of striated planes did not allow to determine a significant tensor. For the others, one or two tensors have been obtained by one or the other method of analysis, each explaining one subset of striae (fig. 10). The analysis of the striae by the inverse method, however, was possible only for 13 stations. The consequence of this is a lack of information in a statistical sense for the ratio of the constraint ellipsoid. The results join those of the global analysis, indicating 2 clearly dis-

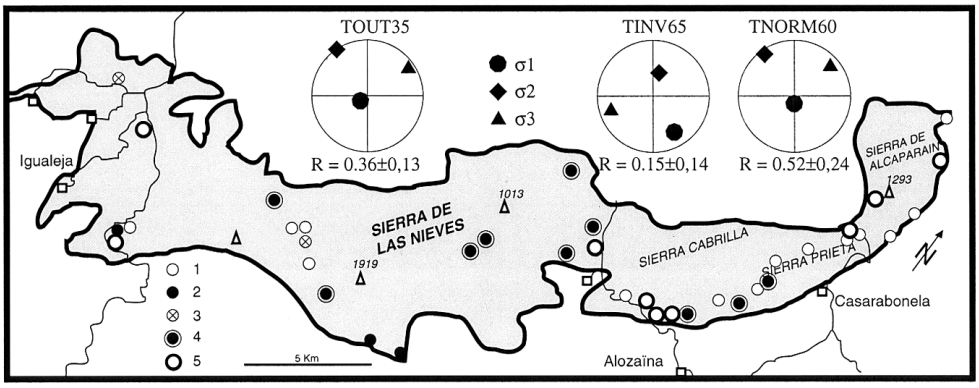

FIG. 8. – Tensors computed using an inverse method for all faults (TOUT35), normal faults (TNORM60) and reverse faults (TINV65). *Distribution of the stations : 1 – comprising faults inconsistent with TOUT35, TNORM60 or TINV65; 2 – comprising faults consistent with TOUT35 only; 3 – comprising faults consistent with TINV65 only; 4 – comprising faults consistent with TOUT35 and TNORM60; 5 – comprising faults consistent with TOUT35, TNORM60 and TINV65.*
FIG. 8. – *Tenseurs obtenus par méthode inverse sur l'ensemble des failles (TOUT35), les failles normales (TNORM60) et les failles inverses (TINV65). Répartition des stations : 1 – ne comportant pas de faille expliquée par TOUT35, TNORM60 ou TINV65 ; 2 – comportant des failles expliquées par TOUT35 seulement ; 3 – comportant des failles expliquées par TINV65 seulement ;* 4 *– comportant des failles expliquées par TOUT35 et TNORM60* ; 5 *– comportant des failles expliquées par TOUT35, TNORM60 et TINV65.*

tinct regimes (fig. 11). The determination of 2 tensors at a single station has solely been possible in 4 cases out of 8. Their succession is hence delicate to establish because the microtectonic criteria are subtle, but the following chronology can be proposed :

– one wrenching phase, at σ1 NW (to NW-SE), brought to the fore at 8 stations (n° 1, 4, 14, 18, 28, 33, 34, 36). Wherever they could be determined, the R ratios have values close to 0.5 (ranging from 0.45 to 0.74), characteristic for a wrenching regime ;

– one extensive phase, brought to the fore at 11 stations (n° 2, 11, 15, 16, 17, 18, 21, 23, 36, 37, 38) with a σ3 close to horizontal and roughly of N-S direction apart from the stations 2 and 11, where it is close to E-W. This can be explained by local effects or permutations of σ2 and σ3 because the R ratios calculated are rather low (0.53 to 0.13 with an average of 0.3), indicating a radial tendency for the extension.

Figure 10 shows an example for the treatment of striae measurements. In this particular case, it is possible to isolate, at the same station, a principal tensor in extension which explains the stria n° 26, as well as a secondary, wrenching tensor, compatible with the stria n° 25. In fact, the stria n° 25 is located on the same fault plane as the stria n° 26, which cuts through the former.

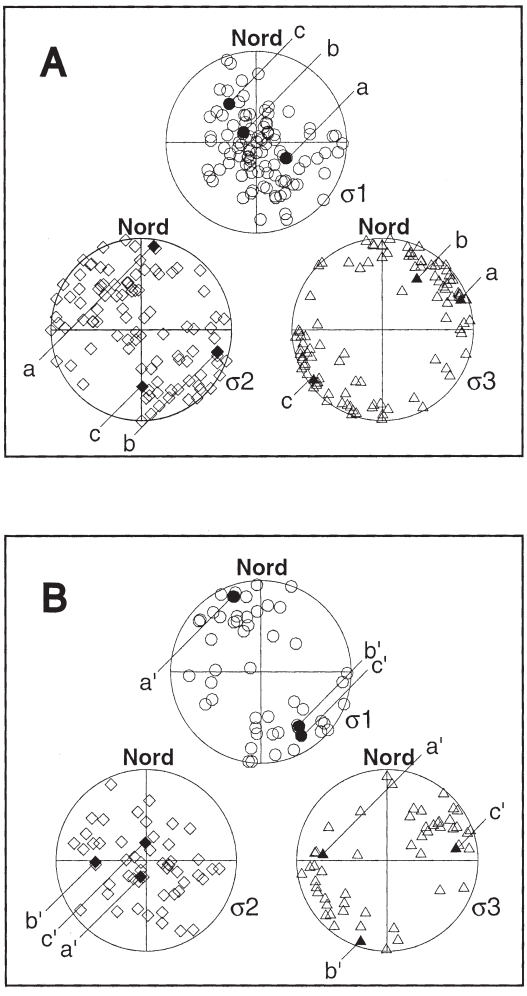

FIG. 9. – Projection of optimal constraints computed (friction angle=30° and R=0,5) from striae measurements.
A : normal faults; B : reverse faults; (a,a') (b,b') (c,c') : pairs of intersecting striae.
FIG. 9. – Projection des contraintes optimales obtenues (angle de frottement=30° et R=0,5) à partir des mesures de stries.
A : failles à composante normale; B : failles à composante inverse ; *(a,a') (b,b') (c,c') : couples de stries sécantes*

INTEGRATION OF THE RESULTS INTO THE REGIONAL GEODYNAMIC CONTEXT

The location of the hydrogeological unit Yunquera-Nieves in the occidental part of the Betic Cordillera endows it with a complex tectonic history linked to the relative irregular movements of Africa and the Iberian Peninsula and, consequently, to the evolution of the occidental Mediterranean Basin. Since the closure of Tethys and the opening of the Atlantic during the Jurassic [Dercourt *et al.,* 1986], the different stages of construction of this domain have been described or discussed by numerous authors [Durand Delga, 1980; Philip, 1987; Rehault, 1981; Martín-Algarra, 1987; De Jong, 1990], revealing the great complexity of the tec-

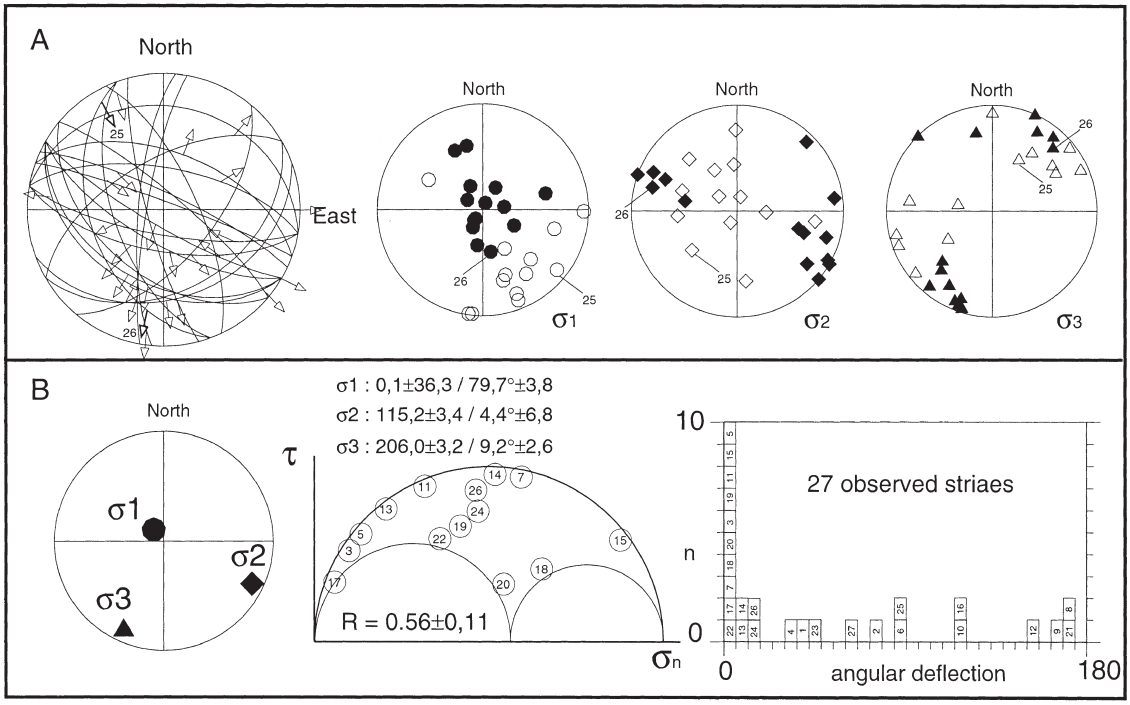

FIG. 10. – Example of a tensor analysis at a station (n° 36).
A : projection (Schmidt diagram) of faults, associated striae and σ1, σ2, σ3 computed for each striae using the optimal constraints method.
B : tensor computed using the inverse method for a set of striae (black dots) : projection of σ1, σ2 and σ3, Mohr circle and histogram of deflections between observed and computed striae.
FIG. 10. – *Exemple d'analyse tensorielle sur une station (n° 36).*
A : *projection (type diagramme de Schmidt) des failles, des stries associées et des σ1, σ2 et σ3 calculés pour chaque strie par la méthode des contraintes optimales.*
B : *tenseur calculé par méthode inverse pour un sous-groupe de stries (points noirs) : projection de σ1, σ2 et σ3, cercle de Mohr et histogramme des écarts entre stries observées et calculées.*

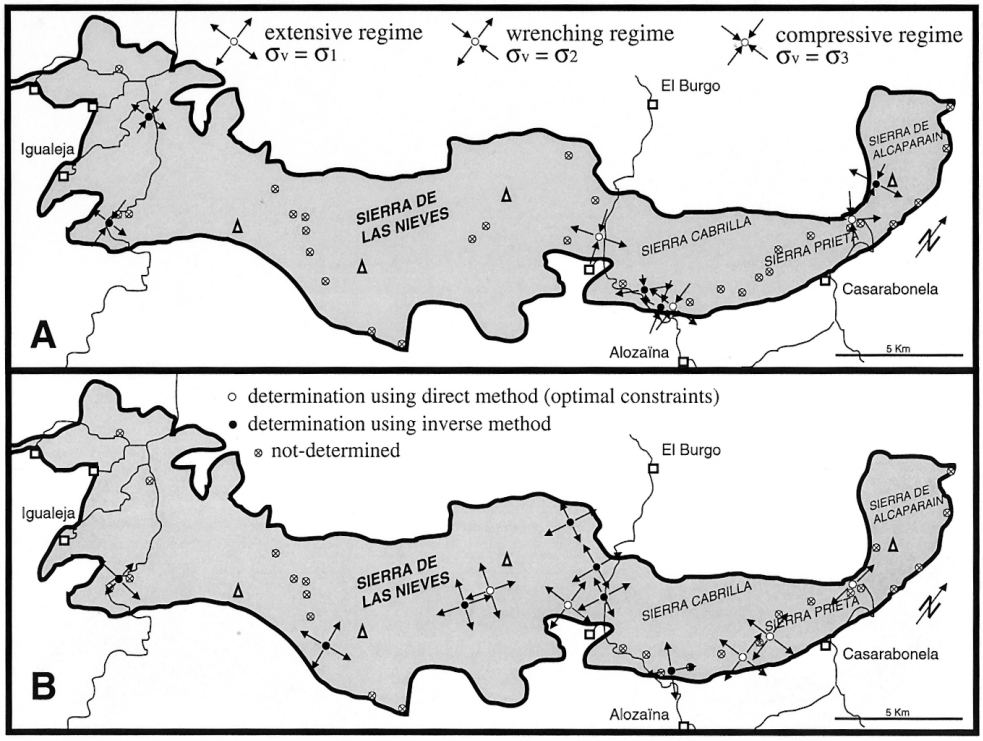

FIG. 11. – Constraint tensors computed for each station.
A : strike-slip tensors (locally compressive)
B : extensive tensors.
FIG. 11. – *Tenseurs de contrainte obtenus par station.*
A : *tenseurs en régime décrochant (localement compressif)*
B : *tenseurs en régime extensif.*

tonic stages and divergences as for their dating. Nevertheless, the following succession shall be proposed :

– in the lower Cretaceous, the development of the Atlantic, which begins during the lower Jurassic, causes the Iberian plate to be dragged by Africa thereby opening the Gulf of Gascogne. The movement of this plate is progressively hindered by the convergence of Africa and Europe. The compression concerns the whole of the Mediterranean in the upper Cretaceous. For the Betic domain, the deformation begins to initiate in overlapping nappes, accompanied by a metamorphism which affects the Internal Zones (I.Z.) ;

– these compressive deformations, locally associated to metamorphism, carry on into the Eocene and reach the External Zones (E.Z.) of the range [Carmignani *et al.*, 1995; Guerrera *et al.,* 1993] ;

– during the Oligocene, the distension extends to Europe through the formation of grabens, generally in N-S extension (Rhine, Rhône), and spreads to the south thereby giving birth to the Algero-Provençal basin ;

– at the beginning of the Miocene, the present structuring in nappes of the Internal Zones terminates. In detail, the Alpujarride complex superposes on the Nevado-Filabride and the Malaguide on the two previous ones [Sanz de Galdeano *et al.,* 1990]. Subsequently, the combined effects of Africa's subduction and the opening of the Algero-Provençal basin cause, initially, the westward expulsion of the I.Z. along with their elongation, and later, at the Burdigalian, a situation where I.Z. and E.Z. collide : the direction of the compression is then NW-SE. After suturing of the contact between I.Z. and E.Z., the direction of the compression becomes WNW-ESE at the Serravalian and rotates once more to become NNW-SSE at the Tortonian (until Messinian) [Ott d'Estevou and Montenat, 1985]. During this entire period, the strike-slip displacements play an important role moving in directions in accordance with the changes of $\sigma 1$. The first regime found in the Yunquera-Nieves unit is equivalent to this compressive wrenching phase.

Until recently, the Miocene tectonic regime was thought to be polyphased while continuously compressive, but recent work [Torres-Roldan *et al.*,1986; Orozco and Crespo-Blanc, 1993; Vissers and Van der Wal, 1993; Crespo-Blanc *et al.*, 1994] resulted in more complex models for this period, including the episodes in extension related to the creation of the Alboran basin [Balanya *et al.*, 1993] ;

– the regime from the end of the Miocene to the beginning of the Quaternary has been considered as globally extensive [Benkhelil, 1976; Groupe de Recherche Néotectonique de l'Arc de Gibraltar, 1977] with a distension approximating N-S which was sufficiently intense to open the Strait of Gibraltar [Benkhelil and Guiraud, 1976] and to engender an important crustal thinning associated with an alkaline volcanism [Van der Beek and Cloetingh, 1992]. But, for the same period, certain authors [Ott d'Estevou and Montenat, 1985; Simon-Gómez, 1986] indicated a regime characterized either by a N-S compression and perpendicular extension or by a radial extension in certain sectors [Jalaboy *et al.*, 1993]. On the slopes of the Sierra Nevada in the region of Granada, Galindo-Zaldívar and González-Lodeiro [1988] noticed a distension phase with a radial tendency, considered as local and related to the isostatic readjustment of the massif [Sanz de Galdeano *et al.*, 1982]. The same type of tensor has been encountered on the border of the Granada basin by Pistre *et al.* [1999], in the carbonate massif of Sierra Gorda. The second regime found in the Yunquera-Nieves unit is consistent with this phase and very similar to that encountered by Andreo *et al.* [1997] on the neighbouring carbonate complex composed of the Sierras Blanca and Mijas ;

– the beginning of the Pleistocene is marked by tectonics characterised by an ENE-WSW to E-W extension [Bousquet and Philip, 1976a], associated with a shortening direction close to N-S. During the early Pleistocene, the regime becomes truly compressive around NW-SE to NNW-SSE directions [Bousquet and Philip, 1976b]. It causes the formation of kilometric folds, reverse and strike-slip faults [Bousquet, 1979; Bousquet and Montenat, 1974]. This regime appears to correspond to the present time regime, which is responsible for the historical seismic activity in this region [Sanz de Galdeano, 1985; Chung and Kanamori, 1976]. A post-middle Quaternary, moderate distensive regime has however been reported locally, comparable to the post-Tortonian to Quaternary one with a lower intensity, though able to generate normal faults or strike-slip displacements [Lhénaff, 1965; Sanz de Galdeano, 1980].

CONSEQUENCES FOR THE CIRCULATION OF FLUIDS

The intensive orogenic phases during the Miocene have favoured the individualisation of the massif and its general structuring, which was completed during the Aquitanian/Burdigalian as witnessed by the breccias of La Nava [Martín-Algarra and Estévez, 1984]. Its structural position, thrusting over the poorly permeable Flysch materials of the Campo de Gibraltar and bordered in the south and east by Alpujarride (peridotites) and Malaguide formations, as well as its synclinal structure explain the general drainage direction and the location of the springs [Liñán *et al.*, 1996; Pistre *et al.*, 1998].

Inside the massif, a major part of the fracturing is likely to be inherited from the first orogenic stages. It represents a dense network along the privileged directions (essentially WSW-ENE and NW-SE, and finally N-S and E-W) which reworked depending on subsequent changes of the tectonic regime. The carbonate unit of Yunquera-Nieves has certainly acquired the essential of its aquifer properties during the post-Tortonian to Quaternary distensive episode whose extension direction appears to situate around NE-SW but shows a radial tendency. It is delicate to propose a precise dating for this phase : it seems to be post-Tortonian and ante-Quaternary. Indeed, the Quaternary regimes which succeeded do not appear intense enough to deform the interior of the compartments in a noticeable way. The radial tendency of this distension regime made most of the pre-existing directional joint families to rework, thereby generating an important overall permeability.

These results corroborate those obtained by Delannoy and Guendon [1998], who distinguish four karstic structuring stages posterior to the end-Burdigalian orogenesis.

– The post-Burdigalian and ante-Messinian period corresponds to the development of a karst of feeble energy, probably beginning immediately after the ablation of the nappes which covered the massif, as witnessed by the first

generation of travertine encountered in the massif e.g. in the sector of Yunquera (fig. 2).

– During the Messinian, the combined effects of the lowered eustatic level, responsible for a differential erosion between the carbonates and the overthrusting formations situated in the SE, but also the instauration of a distensive regime accelerate the karstification and permit the development of vertical structures. Inside the massif, the general hydraulic gradient, conditioned by the structural position of the massif and the direction of the minor constraint NE-SW permitted a preferential karstification along the large, NW-SE and sub-meridian accidents. These accidents have controlled the karstification of the smaller fracturing which has developed in all fracturing directions. Regarding the tectonic history of the massif, the sub-meridian appears as a privileged direction of compression. The associated development of diaclases could explain that, at the present scale, this direction is affected by karstification at a higher degree. These results conform those obtained for a neighbouring carbonate massif by Andreo *et al.* [1997].

– The Pliocene transgression slows down the karstification by augmenting the basic hydraulic level.

– During Quaternary periods, modifications of the hydraulic gradient for tectonic or eustatic reasons as well as modifications of the vegetation cover lead to different periods of karstification. The latter have been recorded by successive travertine depositions [Durán-Valsero, 1996] during hot episodes like during the Pleistocene (Eemian) or the Holocene, and their incisions during the cold episodes of the Riss and Würm in particular. More recently, human activity [Delannoy, 1997] led to a modification of the morphokarstic processes by deforestation.

CONCLUSION

The analysis of fracturing in the hydrogeological unit of Yunquera-Nieves allowed to establish the scheme of the discontinuity network at various scales in a statistical sense as well as to define the role played by tectonics for its evolution. An extensive regime with radial tendency succeeding to a wrenching regime has clearly been brought to the fore. This result assigns a regional character to this probably post-Tortonian to ante-Quaternary regime, since it is compatible with other observations made in neighbouring massifs, which have so far been explained by local stresses. This has an important effect on the geodynamic scheme of the occidental part of the Betic Cordillera : it may indicate a regional isostatic and post-orogenic readjustment.

This extensive stage has had a major effect on the karstification of the reservoir and hence on the acquisition of its hydrodynamic properties. It has enabled the development of a typically karstic “multi-porosity” structure with large drains (NW-SE and sub-meridian) supplied by a network at a smaller scale (fracturing NW-SE and sub-meridian but also E-W and NE-SW).

Considering the study of carbonate reservoirs in highly tectonized domains from a methodological point of view, these results show the influence of regional tectonic regimes on subterranean circulation at a more local scale.

Acknowledgements. – The authors are grateful to F. Cornaton and J.F. Ravel who have made important microtectonic data treatments, B. Célérier (Hydrosciences Laboratory, Montpellier) for advice and access to microtectonic analysis softwares and S. Bottcher for translations.
This work is a contribution of the research group RNM 718 of the Junta de Andalucia to the IGCP 448 project and to the HI 1998-0251 and PB 98-1397 projects of DGESIC.

References

Andreo B., Carrasco F. & Sanz de Galdeano C. (1997). – Types of carbonate aquifers according to the fracturation and the karstification in a southern Spanish area. – *Env. Geology*, **28** (1), 1-11.

Angelier J. & Goguel J. (1979). – Sur une méthode simple de détermination des axes principaux des contraintes pour une population de failles. – *C.R. Acad. Sci.*, Paris, D, **288**, 307-310.

Balanyá J.C., Azañón J.M., Sánchez-Gómez M. & Garciá-Dueñas V. (1993). – Pre-Miocene crustal extension in the Alpujarrides Units and their metamorphic P-T conditions (western Betic Chain). – Abs. meeting Montpellier, March 1993. – *Doc. BRGM*, p. 12.

Benavente-Herrera J. & Sanz de Galdeano C. (1985). – Relación de las direcciones de karstificación y del termalismo con la fracturación en las Cordilleras Béticas. – *Estudios Geol.*, **41**, 177-188.

Benkhelil J. (1976). – Etude néotectonique de la terminaison occidentale des Cordillères bétiques (Espagne). – Thèse 3^{o} cycle, Univ. Nice, France, 353 p.

Benkhelil J. & Guiraud R. (1976). – A propos du style et de l’âge des déformations récentes de la terminaison occidentale des Cordillères bétiques. – *C. R. Acad. Sci.*, Paris, D, **282**, 1339-1342.

Blumenthal M. (1930). – Beitrage zur Geologie der betishen Cordilleren beiderseits des Rio Guadalhorce. – *Eclogae Geol. Helv.*, **23**, 41-293.

Bott M. (1959). – The mechanics of oblique slip faulting. – *Geol. Mag.*, **96** (2), 109-117.

Bourgois J. (1978). – La transversale de Ronda, Cordillères bétiques, Espagne. Données géologiques pour un modèle d’évolution de l’arc de Gibraltar. – Thèse Doct., Univ. Besançon, France, 30, 445 p.

Bousquet J.C. (1979). – Quaternary strike-slip faults in southern Spain. – *Tectonophysics*, **52**, 277-286.

Bousquet J.C. & Montenat C. (1974). – Présence de décrochements nord-est/sud-ouest plio-quaternaires, dans les Cordillères bétiques orientales (Espagne). Extension et signification générale. – *C. R. Acad. Sci.*, Paris, D, **278**, 2617-2620.

Bousquet J.C. & Philip H. (1976a). – Observations microtectoniques sur la compression nord-sud quaternaire des Cordillères bétiques orientales (Espagne méridionale – arc de Gibraltar). – *Bull. Soc. géol. Fr.*, (7), **XVIII**, 3, 711-724.

Bousquet J.C. & Philip H. (1976b). – Observations tectoniques et microtectoniques sur la distension plio-pléistocène ancien dans l’Est des Cordillères bétiques (Espagne méridionale). – *Cuad. Geol. Univ. Granada*, **7**, 57-67.

Carmignani L., Decandia F.A., Disperati L., Fantozzi P.L., Lazzaroto A., Liotta D. & Ogiano G. (1995). – Relationship between the Sardinia-Corsica Provençal Domain and the northern Apennines. – *Terra Nova*, **7**, 2, 128-137.

Célérier B. (1995). – Tectonic regime and slip orientation of reactivated faults. – *Geophys. Jour. Int.,* **121**, 143-191.

Chung W.Y. & Kanamori H. (1976). – Source process and tectonic implications of the Spanish deep-focus earthquake of March 29, 1954. – *Phys. Earth Planet. Inter.*, **13**, 85-96.

Crespo-Blanc A., Orozco M. & García-Dueñas V. (1994). – Extension versus compression during the Miocene tectonic evolution of

the Betic chain late folding of normal fault system. – *Tectonics*, **13**, 1, 78-88.

De Jong K. (1990). – Alpine tectonics and rotation pole evolution of Iberia. – *Tectonophysics*, **184**, 279-296.

Delannoy J.J. (1997). – Recherches géomorphologiques sur les massifs karstiques du Vercors et de la transversale de Ronda; les apports morphogénétiques du karst. – Thèse d'Etat, Univ. Grenoble, France, 678 p.

Delannoy J.J. & Guendon J.L. (1998). – Les apports du karst dans la tectogenèse : exemple de la Serrania de Ronda (Andalousie). – *Spéléochronos*, Hors série, 197-200.

Dercourt J. & 18 others (1986). – Geological evolution of the Tethys belt from the Atlantic to the Pamirs since the Lias. – *Tectonophysics*, **123**, 241-315.

Drogue C., Mas G., Grillot J.C., Lloria C. & Guérin R. (1975). – Utilisation du filtrage optique pour l'étude de la fracturation des roches carbonatées en hydrogéologie. – *Rev. Géog. Phys. Géol. Dyn.*, **XVII** (1), 39-44.

Drogue C. & Costa Almeida C.A. (1984). – Déformations cassantes et structure de magasin dans la couverture carbonatée mésozoïque du centre du Portugal, Est du plateau de Fatima. – *C.R. Acad. Sci.,* Paris, **299**, II, 9, 577-580.

Durán-Valsero J.J. (1996). – Los sistemas karsticos de la provincia de Málaga y su evolución; contribución al conocimiento paleoclimatico del Cuaternario en el Mediterráneo occidental. – Thèse Doct., Univ. Complutense Madrid, Espagne, 409 p.

Durand Delga M. (1980). – La Méditerranée occidentale : étapes de sa genèse et problèmes structuraux liés à celle-ci. – *Mém. H. série Soc. géol. Fr.*, **10**, 203-224.

Dürr S.H. (1967). – Geologie der Serrania de Ronda und ihrer sudwetichen Ausläufer (Andalusien). – *Geol Rom.*, **VI**, 1-73.

Etchécopar A., Vasseur G. & Daignières M. (1981). – An inverse problem in microtectonics for the determination of stress tensor from fault striation analysis. – *J. Struct. Geol*., **3**, 1, 51-65.

Ford D. & Williams P. (1989). – Karst geomorphology and hydrology. – Chapman & Hall ed., 601 p.

Galindo-Zaldívar J. & González-Lodeiro F. (1988). – Faulting phase differentiation by means of computer search on a grid pattern. – *Ann. Tectonicae*, **II**, 2, 90-97.

Grillot J.C. (1979). – Structure des systèmes aquifères en milieu fissuré : contribution méthodologique à cette connaissance. – Thèse d'Etat, Univ. Montpellier, France, 212 p.

Groupe de Recherche Néotectonique de l'arc de Gibraltar (1977). – L'histoire tectonique récente (Tortonien à Quaternaire) de l'arc de Gibraltar et des bordures de la mer d'Alboran. – *Bull. Soc. géol. Fr.*, (7), **XIX**, 3, 575-614.

Guerrera F., Martín-Algarra A. & Perrone V. (1993). – Late Oligocene-Miocene syn-/late orogenic successions in western and central Mediterranean Chains from the Betic Cordillera to the southern Apennines. – *Terra Nova*, **5**, 6, 525-544.

Hoeppener R., Hoppe P., Dürr S.H. & Mollat H. (1964). – Ein querschnitt durch die Betischen Kordilleren bei Ronda (SW Spanien). – *Geol. Mijnb.*, **43**, 282-298.

Jalaboy A., Galindo-Zaldívar J. & González-Lodeiro F. (1993). – The Alpujarride-Nevado-Filabride extensional shear zone, Betic Cordillera, SE Spain. – *J. Struct. Geol*., **15**, 555-569.

Kiraly L. (1975). – Rapport sur l'état actuel des connaissances dans le domaine des caractères physiques des roches karstiques. – Hydrogeology of karstic terrains, A.I.H., 53-67.

Lhénaff R. (1965). – Néotectonique quaternaire sur le bord occidental de la Sierra Nevada (province de Grenade, Espagne). – *Rev. Géog. Phys. Géol. Dyn*., **VII** (3), 205-207.

Liñán C., Carrasco F. & Andreo B. (1996). – Transito aguas bajas-aguas altas en la unidad hidrogeológica Yunquera-Nieves. – *IV SIAGA*, Almería, 271-280.

Martín-Algarra A. & Estévez A. (1984). – La brèche de la Nava : dépôt continental synchrone de la structuration pendant le Miocène inférieur des zones internes de l'Ouest des Cordillères bétiques. – *C. R. Acad. Sci*., Paris, **299**, II, 8, 463-466.

Martín-Algarra A. (1987). – Evolución geológica alpina del contacto entre las Zonas internas y las Zonas externas de la Cordillera Bética. – Thèse Doct., Univ. Granada, Espagne, 1171 p.

Orozco M. & Crespo-Blanc A. (1993). – Extension during orogen building. The contraviesa detachment fault system (Betic Cordilleras, southern Spain). – Abs. meeting Montpellier – March 1993. – *Doc. BRGM*, 156-157.

Ott d'Estevou P. & Montenat C. (1985). – Evolution structurale de la zone bétique orientale (Espagne) du Tortonien à l'Holocène. – *C.R. Acad. Sci.*, Paris, **300**, II, 8, 363-368.

Philip H. (1987). – Plio-Quaternary evolution of the stress field in Mediterranean zones of subduction and collision. – *An. Geophys.*, **5B** (3), 301-320.

Pistre S., Liñán C., Andreo B., Carrasco F. & Drogue C. (1998). – Fracturation et karstification du massif de Yunquera-Nieves dans le contexte structural de la Cordillère bétique. – *Spéléochronos*, hors série, 141-144.

Pistre S., López-Chicano M., Pulido-Bosch A. & Drogue C. (1999). – The role of the western Mediterranean tectonic evolution in the geometry of a karstic domain in the Betic Cordilleras (Sierra Gorda, Spain) : importance of a tardy extensional regime. – *Geodin. Acta*, **12** (1), 11-24.

Quinif Y., Vandycke S. & Vergari A. (1997). – Chronologie et causalité entre tectonique et karstification. L'exemple des paléokarsts crétacés du Hénaut (Belgique). – *Bull. Soc. géol. Fr.*, **168**, 4, 463-472.

Rehault J.P. (1981). – Evolution tectonique et sédimentaire du bassin ligure (Méditerranée occidentale). – Thèse Doct. Etat, Univ. Paris VI, France.

Ritz J.F. (1991). – Evolution du champ de contraintes dans les Alpes du sud depuis la fin de l'Oligocène – Implications sismotectoniques. – Thése Doct., Univ. Montpellier, France, 187 p.

Robertson A.H.F. & Grasso M. (1995). – Overview of the late Tertiary tectonic and paleo-environmental development of the Mediterranean region. – *Terra Nova*, **7**, 2, 114-127.

Sanz de Galdeano C. (1980). – La neotectonica del norte de la depresion de Granada. – *Estudios Geol*., **36**, 255-261.

Sanz de Galdeano C., Vidal F. & De Miguel F. (1982). – El sistema de fracturas de direccion N10-30E del borde occidental de la Sierra Nevada (Cordilleras Béticas). – *Estudios Geol*., **38**, 392-398.

Sanz de Galdeano C. (1983). – Los accidentes y fracturas principales de las Cordilleras Béticas. – *Estudios Geol*., **39**, 157-165.

Sanz de Galdeano C. (1985). – La fracturacion del borde sur de la depresion de Granada (Discusion acerca del escenario del terremoto del 25-XII-1884). – *Estudios. Geol*., **41**, 59-68.

Sanz de Galdeano C., Rodríguez-Fernández J. & López-Garrido A.C. (1990). – Les Cordillères Bétiques dans le cadre géodynamique néoalpin de la Méditerranée occidentale. – *Riv. It. Paleont. Strat*., **96**, 2-3, 191-202.

Sanz de Galdeano C. (1990). – Geologic evolution of the Betic Cordilleras in the western Mediterranea, Miocene to present. – *Tectonophysics*, **172**, 107-119.

Simón-Gómez J.L. (1986). – Analisis of a gradual change in stress regime (example from the eastern Iberian chain, Spain). – *Tectonophysics*, **124**, 37-53.

Tapponier P. (1977). – Evolution tectonique du système alpin en Méditerranée : poinçonnement et écrasement rigide-plastique. – *Bull. Soc. géol. Fr.*, (7), **XIX**, 3, 437-460.

Torres-Roldán R., Poli G. & Peccerillo A. (1986). – An early Miocene arc-tholeitic magmatic dike event from the Alboran sea : evidence for precollisional subduction and back-arc crustal extension in the western Mediterranea. – *Geol. Rundsch*., **75**, 219-234.

Van der Beek P.A. & Cloetingh S. (1992). – Lithospheric flexure and the tectonic evolution of the Betic Cordilleras (SE Spain). – *Tectonophysics*, **203**, 325-344.

Vissers R.L.M. & Van der Wal D. (1993). – Geology of the Betic lithosphere : Evidence for extensional collapse in the Alboran realm. – Abs. meeting Montpellier, Mars 1993. – *Doc. BRGM*, 204-205.